Expanded View Figures

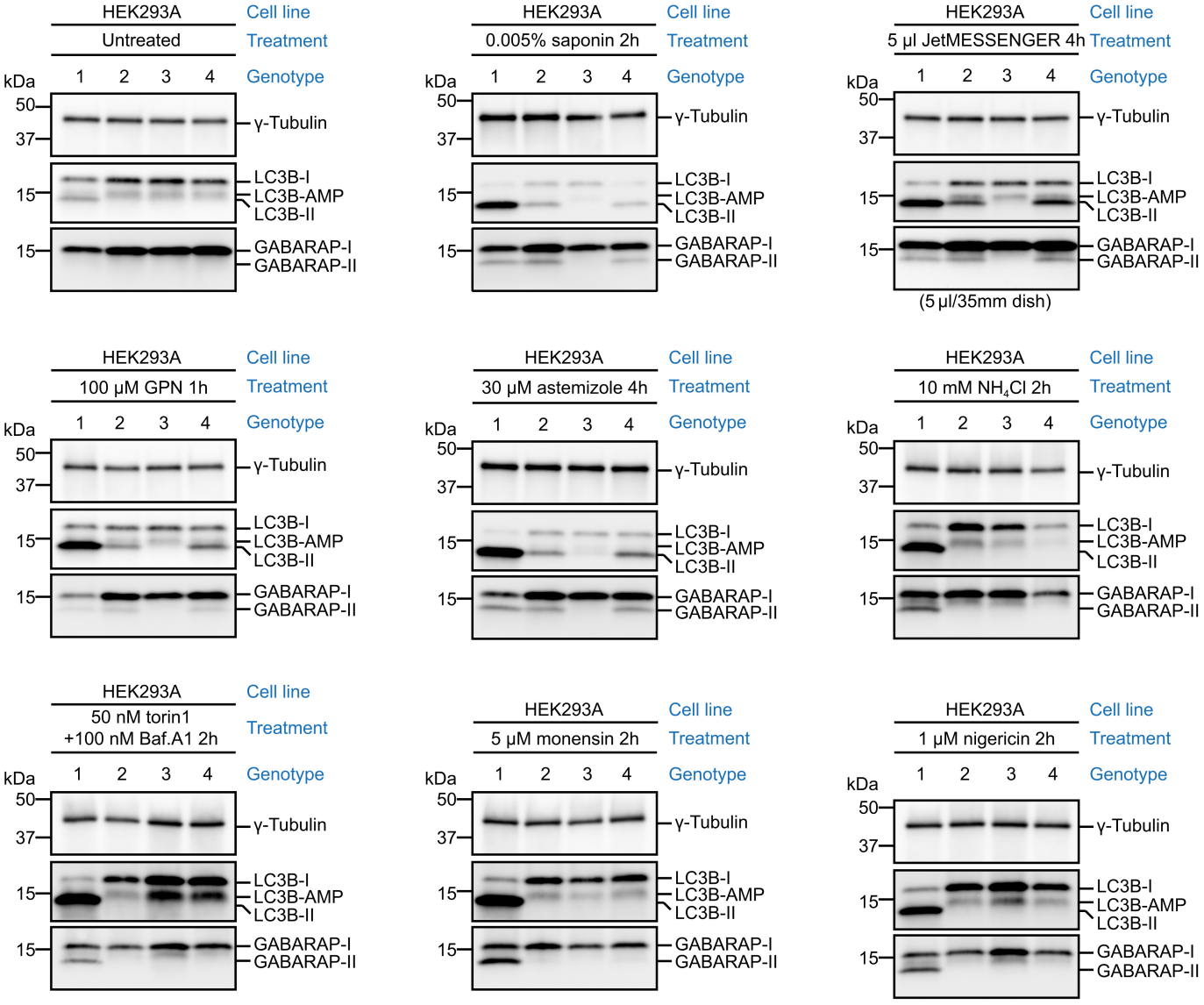

1. WT
2. ATG16L1-KO
3. ATG16L1/TECPR1-DKO
4. ATG16L1/TECPR1-DKO + untagged-TECPR1

Figure EV1. Screening for TECPR1 E3-activity-inducing treatments.

LC3B/GABARAP lipidation in WT, ATG16L1-KO and ATG16L1/TECPR1-DKO HEK293A cells with or without untagged-TECPR1 rescue, treated as indicated. Cell lysates were immunoblotted against the indicated proteins. γ-Tubulin is a loading control.

Figure EV2. The role of V-ATPase in TECPR1 recruitment to damaged lysosomes.

A HEK293A cells transiently transfected with GFP-SidK (aa1-278) treated as indicated for 1 h. Cells were prepermeabilized with 0.05% Saponin on ice for 5 min to eliminate any SidK that was not involved in a membrane-bound complex before cell lysis. The cell lysates were then subjected to GFP-Trap immunoprecipitation, and the input, flowthrough (FT), and bound material were immunoblotted against the indicated proteins.

B Schematic representation of the interaction between GFP-SidK (aa1-278) and the soluble V1 region of the V-ATPase before and after assembly with the membrane-embedded VO region. The diagram highlights the protein components that are lost when the cells are subjected to prepermeabilization. The postassembly state shows the complete V-ATPase complex, including both the V1 and VO regions, interacting with GFP-SidK. Highlighted is also the previously shown interaction with ATG16L1.

C Confocal images of HeLa WT cells transiently transfected with EGFP-SidK, with or without prepermeabilization, treated or not with LLOMe for 1 h as indicated and costained for LAMP1. Scale bars: 10 μm.

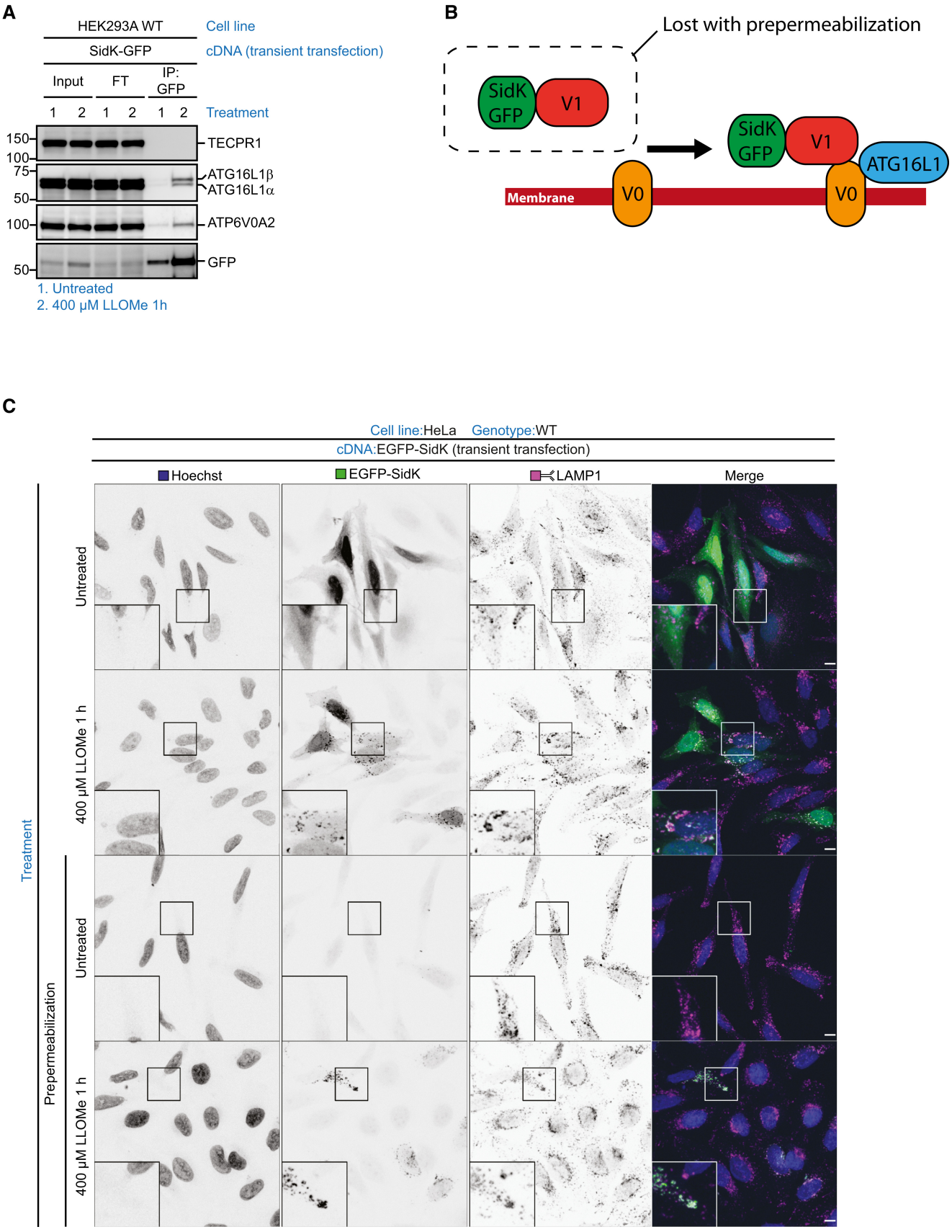

Figure EV2.

Figure EV3. Characterization of LC3B and TECPR1 puncta induced by MC3 and LLOMe.

A–D Confocal images of ATG16L1/TECPR1-DKO HeLa cells expressing mScarlet-LC3B and EGFP-TECPR1, treated as indicated and costained for (A) LAMP1, (B) Ubiquitin, (C) SQSTM1, and (D) Galectin3.

E Confocal images of ATG16L1/TECPR1-DKO HeLa cells expressing EGFP-TECPR1 and costained for LAMP1. Scale bars: 10 μm.

F *Left*: Violin plot displaying the mean number of TECPR1 (left *Y*-axis) and LAMP1 (right *Y*-axis) puncta with treatments as indicated in (E). *Right*: Beeswarm-Superplot displaying %TECPR1 overlapping with LAMP1 in the images represented in (E) quantified by automated analysis using CellProfiler. Mean ± SEM from each independent experiment (3/group) presented as large data points, with the black line corresponding to the mean of means. Individual data points (small) corresponding to single images are color-coded and superimposed according to the biological replicate they originated from. *Both*: Total cells per condition/ images per condition: 2961/72 (untreated) and 2546/75 (30-min LLOMe) were analyzed (*P*-values determined using Student's *t*-test; ns = not significant).

G Confocal images of ATG16L1/TECPR1-DKO HeLa cells expressing EGFP-TECPR1 and costained for both LAMP1 and EEA1. Arrowheads overlay puncta of interest. Scale bars: 10 μm.

H Confocal images of ATG16L1/TECPR1-DKO HeLa cells expressing EGFP-TECPR1 and mCherry-ATG16L1, treated as indicated. Scale bars: 10 μm.

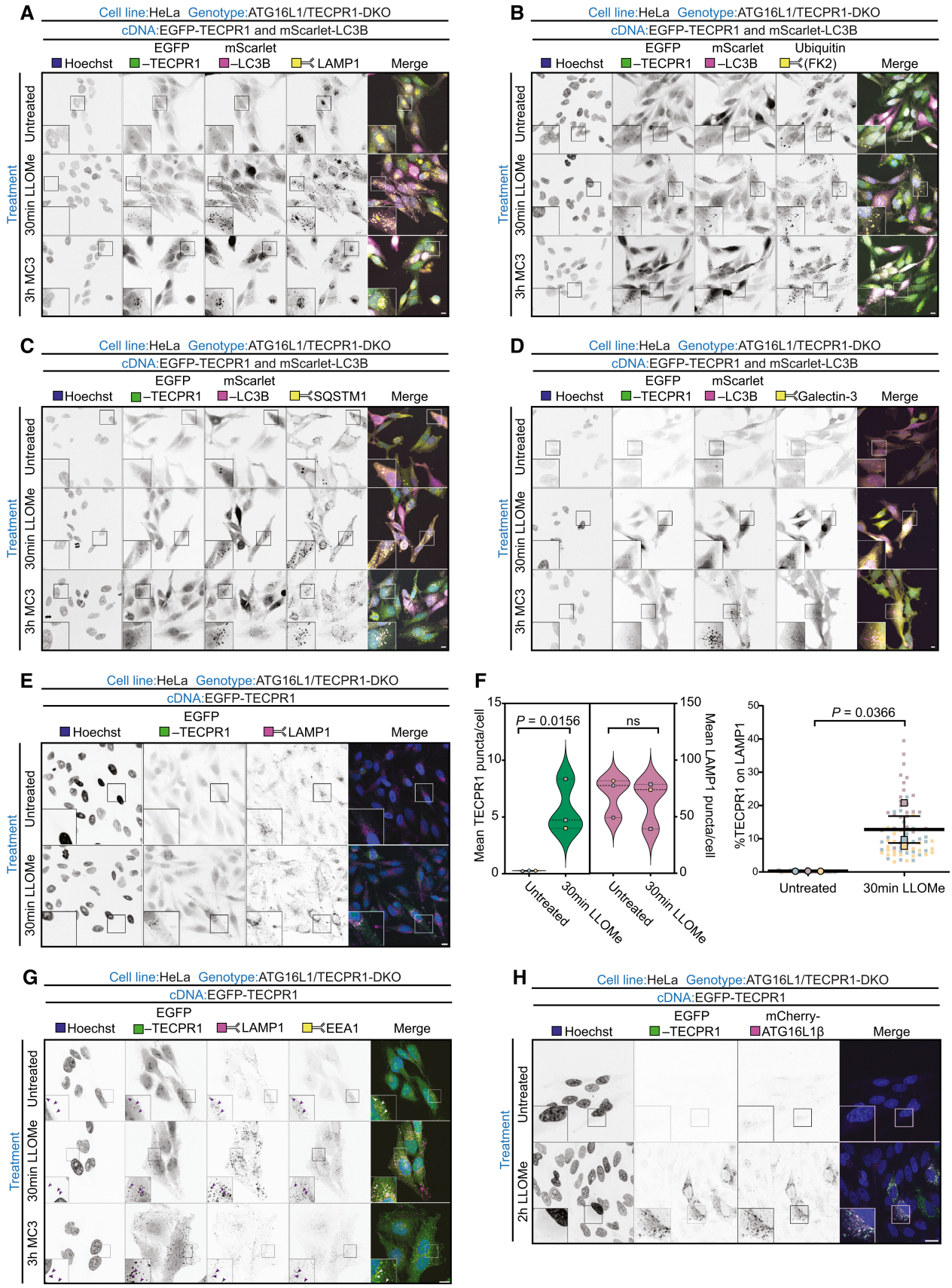

Figure EV3.

Figure EV4. *In vitro* characterization of TECPR1 activity on all ATG8 proteins with PE and PS substrate.

A Table showing lipid composition of liposomes used in (B) and (C).

B Coomassie-stained gel depicting *in vitro* LC3B/GABARAP lipidation reactions facilitated by ATG16L1 using the indicated combinations of proteins and liposomes (with or without SM), after being subjected to a liposome co-sedimentation assay. Separation of reactions into membrane bound (pellet) and supernatant allows clear distinction of ATG8-II and ATG8-AMP.

C The extent of LC3B/GABARAP-I to -II conversion in (A) was determined and plotted as percentage of total LC3B.

D Coomassie-stained gel depicting *in vitro* LC3B/GABARAP lipidation reactions facilitated by TECPR1 using the indicated combinations of proteins and liposomes (with or without SM), after being subjected to a liposome co-sedimentation assay. Separation of reactions into membrane bound (pellet) and supernatant allows clear distinction of ATG8-II and ATG8-AMP.

E The extent of LC3B/GABARAP-I to -II conversion in (A) was determined and plotted as percentage of total LC3B.

A

	PC	PE	PS	Chol	SM
no SM	40%	20%	20%	20%	0%
full mix	30%	20%	20%	20%	10%
no PS	50%	20%	0%	20%	10%
no PE	50%	0%	20%	20%	10%
no PS/PE	70%	0%	0%	20%	10%

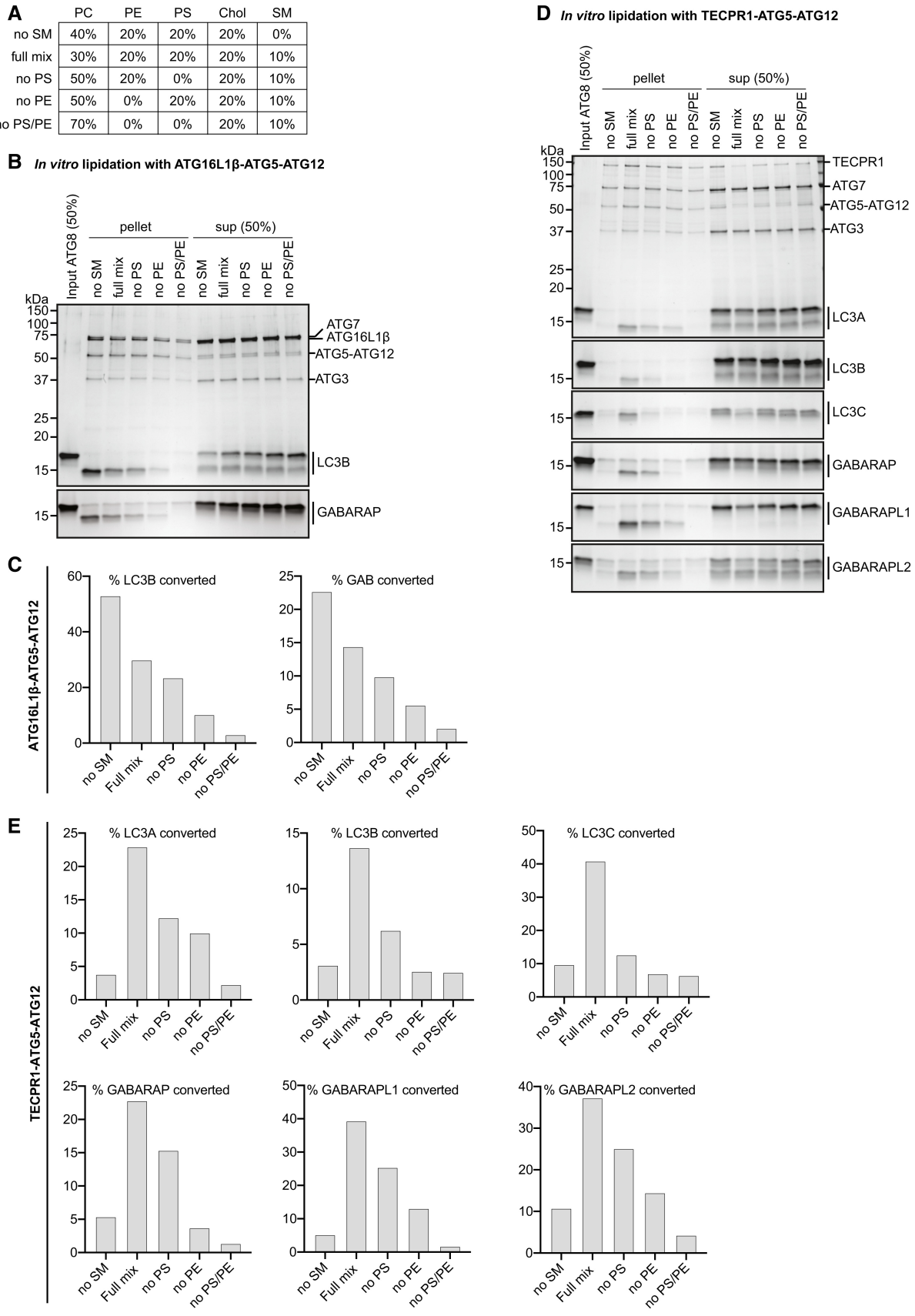

Figure EV4.

Figure EV5. TECPR1 and PtdIns4P converge on damaged lysosomes independently.

A Cell lysates of HeLaK WT and PI4K2α KO cells were immunoblotted for the indicated proteins. Vinculin is a loading control.

B Representative time series of live-cell fluorescence imaging showing redistribution of mCherry-2xSidM (PtdIns4P probe) in HeLaK WT and PI4K2α KO cells following treatment with 400 μM LLOMe. Scale bar: 10 μm.

C Representative time series of live-cell fluorescence imaging showing redistribution of mNG-TECPR1 in HeLaK WT and PI4K2A KO cells following treatment with 400 μM LLOMe. Scale bar: 10 μm.

D Beeswarm-Superplot displaying mean mNG-TECPR1 dots per cell per image represented in (C) quantified by automated analysis using CellProfiler. Mean ± SEM from each independent experiment (3/group) presented as large data points, with the black line corresponding to the mean of means. Individual data points (small) corresponding to single images are color-coded and superimposed according to the biological replicate they originated from. Total cells per condition/images per condition: 2425/43 (WT untreated), 1989/45 (WT LLOMe), 2152/44 (PI4K2A KO untreated), and 2651/43 (PI4K2A KO LLOMe) were analyzed (Data have skewed distribution; *P*-value from Kruskal–Wallis followed by Dunn's multiple comparisons test; ns = not significant).

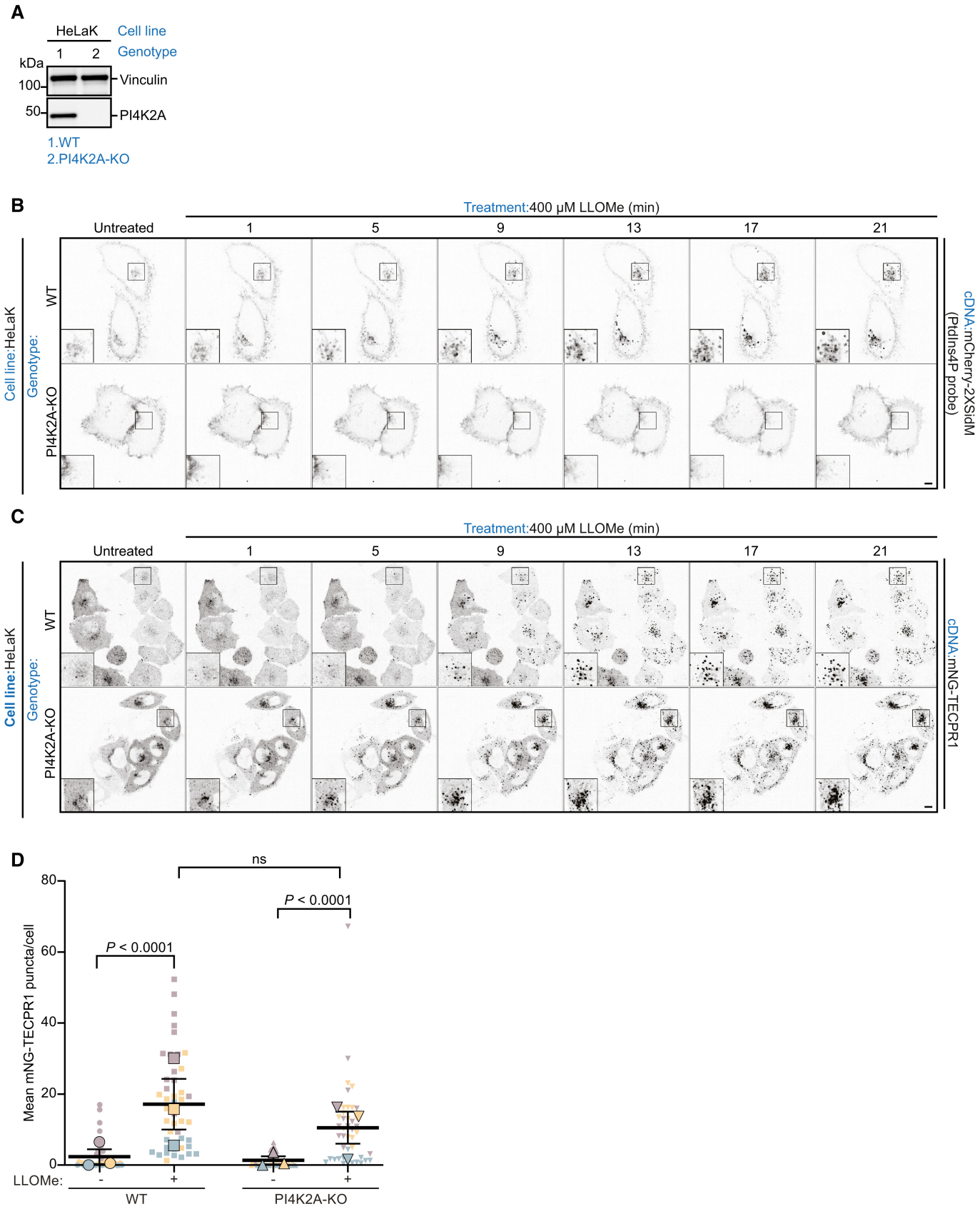

Figure EV5.